Supporting Information for

Electron-beam-evaporated NiO_X for efficient and stable semi-transparent perovskite solar cells and modules

Junye Pan[1], Jiahui Chen[1], Bingxin Duan[1], Yuxi Zhang[1], Peiran Hou[1], Yanqing Zhu[1], Min Hu[2]*, Wangnan Li[3], Yi-Bing Cheng[4], Jianfeng Lu[1]*

[1] State Key Laboratory of Silicate Materials for Architectures, Wuhan University of Technology, Wuhan 430070, China;

[2] School of Electronic and Electrical Engineering, Hubei Province Engineering Research Center for Intelligent Micro-Nano Medical Equipment and Key Technologies, Wuhan Textile University, Wuhan 430200, China;

[3] Hubei Key Laboratory of Low Dimensional Optoelectronic Material and Devices, Hubei University of Arts and Science, Xiangyang 441053, China;

[4] State Key Laboratory of Advanced Technology for Materials Synthesis and Processing, Wuhan University of Technology, Wuhan 430070, China;

* E-mail: jianfeng.lu@whut.edu.cn (JL)

TABLE OF CONTENTS

Experimental section

Materials

All materials in this experiment were used as received without any further purification. Fluorine doped tin oxide (FTO, ca. 10 Ω sq^{-1}) glass was purchased from Yingkou Opv Tech New Energy Technology Co., Ltd.. Hydrochloric acid (HCl) was purchased from China National Pharmaceutical Group Corp.. Urea was purchased from Alfa Aesar. $SnCl_2•2H_2O$ was purchased from Aladdin. Lead bromide ($PbBr_2$), cesium bromide (CsBr), Poly[bis(4-phenyl)(2,4,6-triMethylphenyl)aMine] (PTAA) and poly(3-hexylthiophene) (P3HT) were purchased from Xi'an Yuri Solar Co., Ltd. Thioglycolic acid, 2,2',7,7'-tetrakis[N,N-di(4-methoxyphenyl)amino]-9,9'-spirobifluorene (spiro-OMeTAD), chlorobenzene (CB), toluene, 4-tert-butylphenol (tBP), molybdenum oxide (MoO_X), lithium bis(trifloromethanesulfonyl) imide (LiTFSI) and tris(2-(1H-pyrazol-1-yl)-4-tert-butyl pyridine)-cobalt(III)tris(bis(trifluoromethylsulfonyl)imide)) (FK209) were purchased from Sigma-Aldrich. Nickel oxide (NiO_X) particles and ITO target were purchased from ZhongNuo Advanced Material Technology Co., Ltd..

Device fabrication

Small-area solar cell with spiro-OMeTAD|MoO_X: Firstly, FTO glasses were etched via a femtosecond laser machine (Universal Laser Systems, VLS2.30) and brushed by a toothbrush. Then, they were successively immersed into detergent, deionized water and ethanol for ultrasonic washing (15 min) and dried by dry-air blowing.

Next, SnO_2 electron transport layers (ETLs) were prepared on the FTO surface treated with UV ozone (15 min) by chemical bath deposition (CBD) method as the following steps: (1) 5 mL HCl, 5 g urea, 1.096 g $SnCl_2•2H_2O$ and 100 μL thioglycolic acid were dissolved in 400 mL deionized water to prepare SnO_2 solution with a concentration of 0.012 mol L^{-1} and then stored in a refrigerator for 3 h. (2) A as-cleaned FTO glass was immersed into the SnO_2 solution which was diluted to 0.002 mol L^{-1} for 2.5 h at 83 °C, and then rinsed with deionized water and dried by dry-air blowing. (3) Above substrate was annealed at 180 °C for 1 h.

The $CsPbBr_3$ films were prepared by the following steps: (1) CsBr and $PbBr_2$ powders were thermally evaporated onto the SnO_2 surface with deposition rates of ~3.5 and ~4.5 Å s^{-1} sequentially. The above step was repeated twice. (2) The obtained CsBr|$PbBr_2$ film was annealed at 320 °C for 20 min, and then 300 °C for 40 min.

A hole transport layer (HTL) solution was prepared by dissolving 73 mg spiro-OMeTAD into 1 mL CB followed by additing 30 μL tBP, 18 μL LiTFSI (520 mg mL^{-1} solution in acetonitrile) and 29 μL FK209 (300 mg mL^{-1} solution in acetonitrile). 25 μL spiro-OMeTAD solution was coated on

perovskite film at 3000 rpm for 30 s with a ramp of 1000 rpm s^{-1}. MoO_X powder was thermally evaporated with a rate of 0.1 Å s^{-1} onto the spiro-OMeTAD surface.

Finally, 180 nm ITO electrode was deposited at 37 W by radio frequency (RF) sputtering system under a pressure of 3.75×10^{-5} Torr.

Small-area solar cell with buffer layer|NiO_X: The FTO|SnO_2|$CsPbBr_3$ substrate was prepared according to the above methods.

Various buffer layers were prepared by the following methods: (1) P3HT buffer layer solutions were prepared by dissolving 1/2/5 mg P3HT into 1 mL CB. 25 µL P3HT solution was coated on the perovskite film at 3000 rpm for 30 s with a ramp of 1000 rpm s^{-1}. (2) PTAA buffer layer solution was prepared by dissolving 5 mg PTAA into 1 mL toluene. 25 µL PTAA solution was coated on the perovskite film at 3000 rpm for 30 s with a ramp of 1000 rpm s^{-1}. (3) MoO_X powder was thermally evaporated with a rate of 0.1 Å s^{-1} onto the surface of perovskite film to prepare 5 nm MoO_X buffer layer.

NiO_X were evaporated by electron beam onto the $CsPbBr_3$|buffer layer at the rate of 0.1, 0.2 and 0.3 Å s^{-1} successively to deposit 35 nm NiO_X film. The obtained film was treated at 300 °C for 60 min.

Eventually, 180 nm ITO electrode was deposited at 37 W by RF sputtering system under a pressure of 3.75×10^{-5} Torr.

*Large area perovskite solar module:*Firstly, FTO glasses were etched via a femtosecond laser machine to form P1 lines and then cleaned following the above protocols. SnO_2 and $CsPbBr_3$ film were prepared successively by above methods. For module preparation, the P3HT was deposited by a slot-die coating process in air according to our previous established protocols.[1] The gap between coating head and substrate was fixed to 150 µm. The concentration of P3HT solution was 2 mg mL^{-1} and the coating speed was 8 mm s^{-1} with a pumping speed of 5 µL s^{-1}. After the deposition of the P3HT and NiO_X films, the samples were re-etched to form P2 lines. Eventually, 180 nm ITO electrode was deposited at 37 W by RF sputtering system under a pressure of 3.75×10^{-5} Torr and effective series connected modules were formed via separate the ITO to form P3 lines.

Characterization:

Current density-voltage (J-V) curves of various devices were measured via a source meter of Keithley 2400 and an Oriel solar simulator equipped with a xenon lamp (100 mW cm^{-2}, calibrated by a standard silicon reference solar cell) and an AM 1.5G filter in the room environment. Metal masks with the aperture of 0.16 cm^2 and 10.0 cm^2 for small-area solar cells and large-area solar modules respectively were used to define the active area. The *J–V* scans were recorded at 10 mV steps with a scan rate of 100 mV s^{-1} from 1.6 V to -0.1 V.

Incident photon to current conversion efficiency (IPCE) spectra was measured via a QEX10 solar cell instrument and a photodiode used to calibrate the measurements had been calibrated via Newport.

Quasi-stabilized power output (*q*-SPO) curves were measured via a source meter of Keithley 2400 and an Oriel solar simulator equipped with a xenon lamp (100 mW cm^{-2}, calibrated by a standard silicon reference solar cell) and an AM 1.5G filter in the room environment and recorded at the potential around the maximum power point for 120 s.

Scanning Electron Microscopy (SEM) images were recorded via the Hitachi S4800 and Zeiss Gemini 300.

X-ray diffraction (XRD) patterns were obtained via the Bruker D8 Advance diffractometer equipped with a Cu Ka X-ray tube operated at 40 kV and 40 mA using a step size of 0.02° and a time per step of 0.12 s.

Ultraviolet–visible (UV−Vis) absorption spectra were obtained via UV-vis spectrophotometer (lambda 750S, PerkinElmer).

Steady-state photoluminescence (PL) and time-resolved PL (TRPL) decay curves were measured via the Delta Flex Flux Fluorescence Lifetime System (HORIBA Scientific Company, Japan) with 485 nm laser excitation.

Space charge limited current (SCLC) was measured via a Chenhua electrochemistry workstation in the dark.

Dark J-V curves were measured via a Keithley 2400 source meter and recorded at 10 mV steps with a scan rate of 100 mV s^{-1} from 1.6 V to -0.1V in the dark.

Transient photovoltage (TPV) and transient photocurrent (TPC) tests were used to record the attenuation process of photovoltage and photocurrent.

Mott-Schottky analyses were measured via an impedance spectrum analyzer (Chenhua) in the dark and the frequency is set at 999.682 Hz.

Environmental stability test: According to the protocol of ISOS-D-2, the non-encapsulated small-area solar cells were aged at the condition with a temperature of 65 °C and a relative humidity (RH) of 55 ± 10% in the dark and regularly measured *J-V* curves. According to the protocol of ISOS-D-1, the non-encapsulated large-area solar modules were aged at the condition with a temperature of 25 ± 5 °C and a RH of 35 ± 5% in the dark and regularly measured *J-V* curves.

Heat-insulating performance were measured via an Oriel solar simulator equipped with a xenon lamp (100 mW cm^{-2}, calibrated by a standard silicon reference solar cell) and an AM 1.5G filter in the room environment.

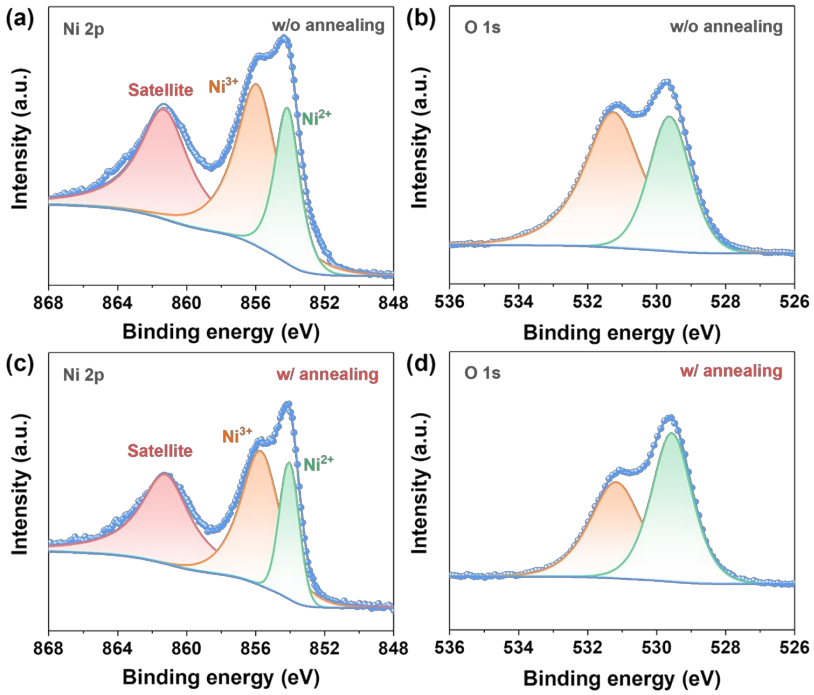

Figure S1. XPS spectra of (a) Ni 2p, and (b) O 1s of NiO_X film without annealing. XPS spectra of (c) Ni 2p, and (d) O 1s of NiO_X film with annealing in air condition.

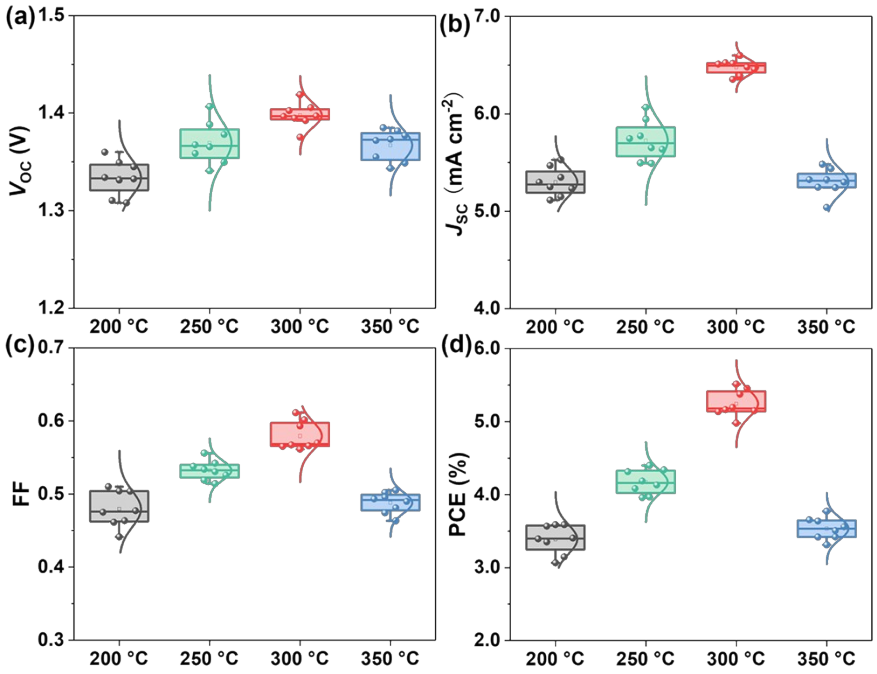

Figure S2. Statistics (a) V_{OC}, (b) J_{SC}, (c) FF, and (d) PCE distributions of 8 independent cells of ST-PSCs based on NiO_X with different annealing temperature. All devices were measured under AM 1.5G 1-sun irradiation with a metal mask of 0.16 cm^2.

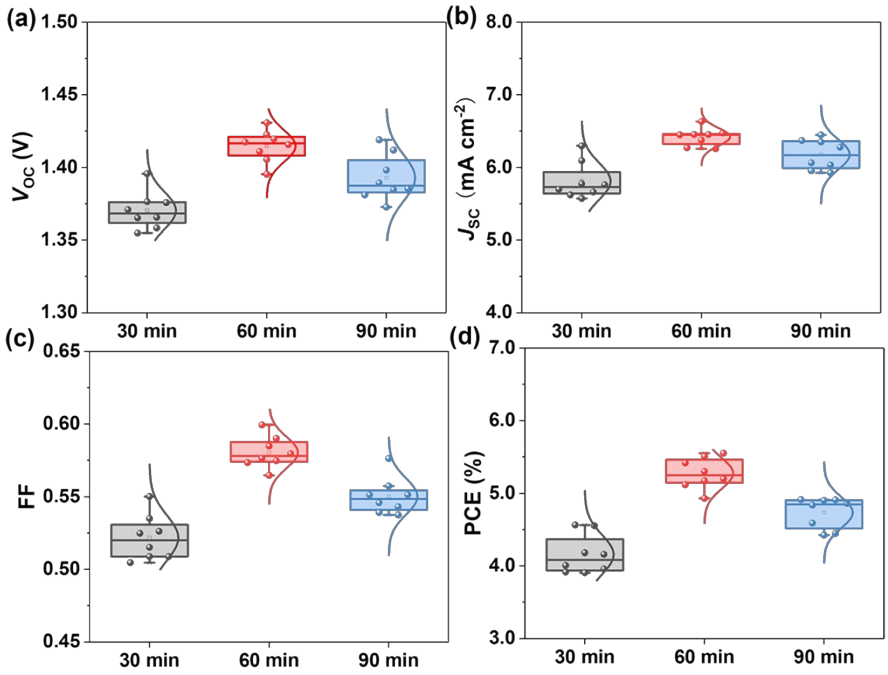

Figure S3. Statistics (a) V_{OC}, (b) J_{SC}, (c) FF, and (d) PCE distributions of 8 independent cells of ST-PSCs based on NiO_X with different annealing time. All devices were measured under AM 1.5G 1-sun irradiation with a metal mask of 0.16 cm^2.

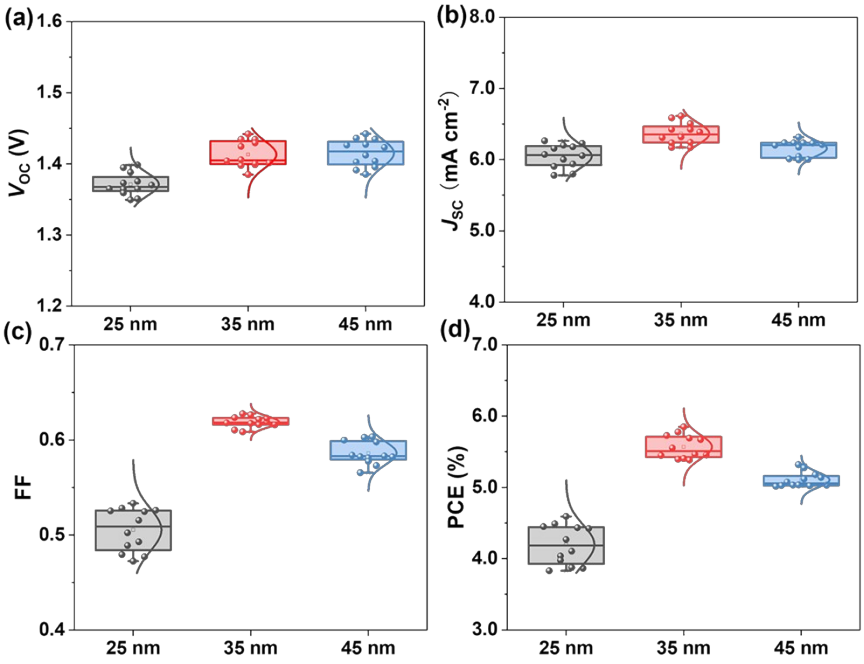

Figure S4. Statistics (a) V_{OC}, (b) J_{SC}, (c) FF, and (d) PCE distributions of 12 independent cells of ST-PSCs based on NiO_X with different thickness. All devices were measured under AM 1.5G 1-sun irradiation with a metal mask of 0.16 cm^2.

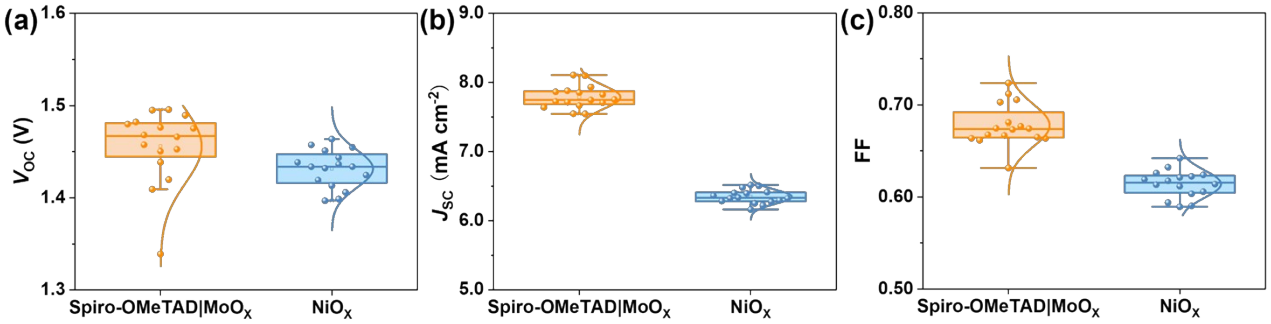

Figure S5. Statistics (a) V_{OC}, (b) J_{SC}, and (c) FF distributions of 16 independent cells of ST-PSCs with spiro-OMeTAD|MoO_X or NiO_X film. All devices were measured under AM 1.5G 1-sun irradiation with a metal mask of 0.16 cm^2.

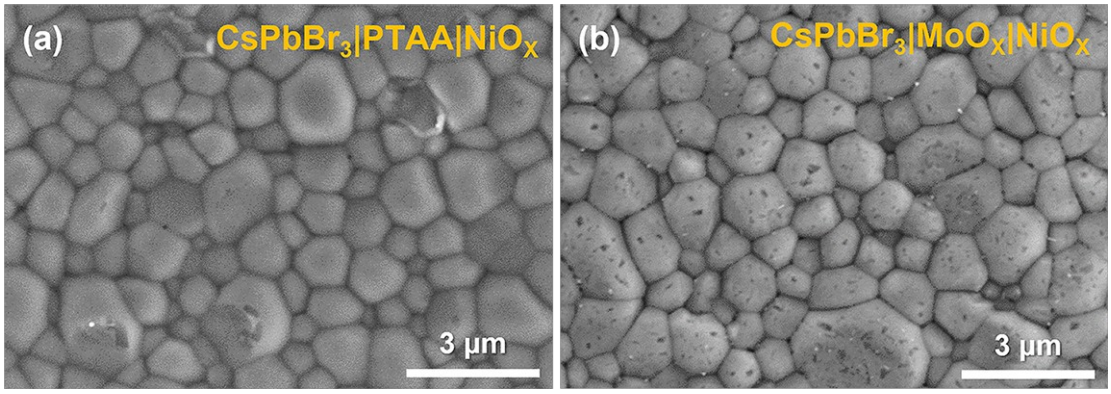

Figure S6. Top-view SEM images of (a) FTO|SnO_2|$CsPbBr_3$|PTAA|NiO_X, (b) FTO|SnO_2|$CsPbBr_3$|MoO_X|NiO_X films.

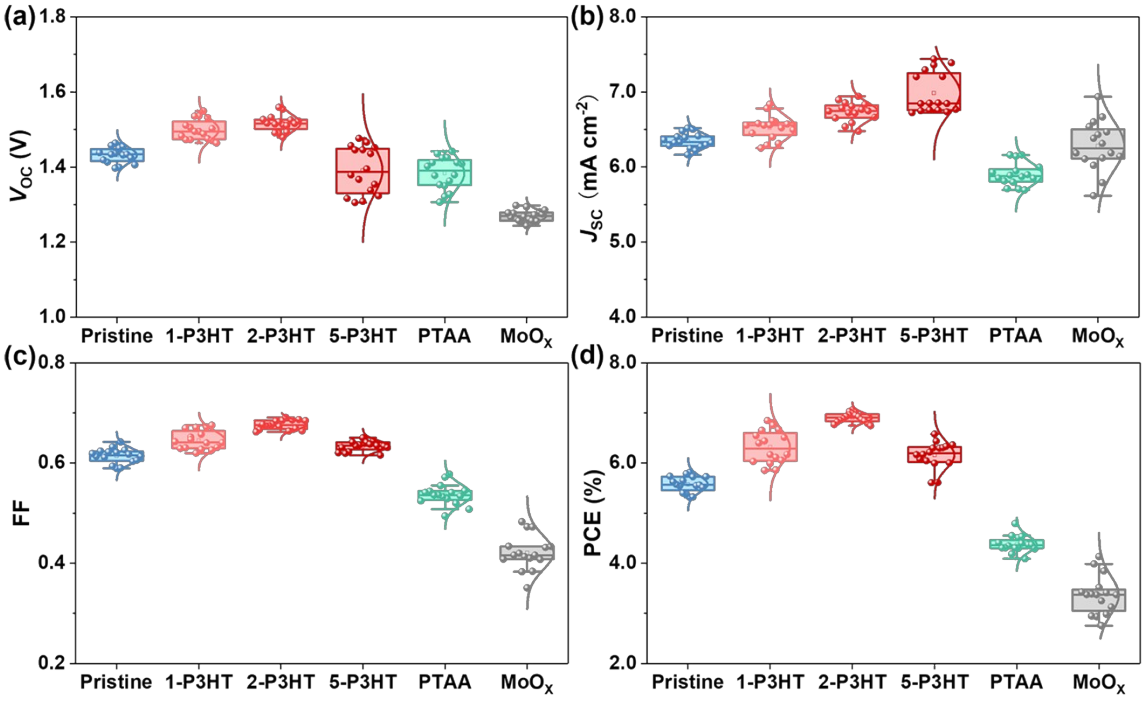

Figure S7. Statistics (a) V_{OC}, (b) J_{SC}, (c) FF, and (d) PCE distributions of 16 independent cells of ST-PSCs with different buffer layers. The device structure is glass|FTO|SnO_2|$CsPbBr_3$|buffer layer|NiO_X|ITO. These buffer layers are fabricated based on 1 mg mL^{-1} P3HT (1-P3HT), 2 mg mL^{-1} P3HT (2-P3HT), 5 mg mL^{-1} P3HT (5-P3HT), 5 mg mL^{-1} PTAA, and 5 nm MoO_X, respectively. All devices were measured under AM 1.5G 1-sun irradiation with a metal mask of 0.16 cm^2.

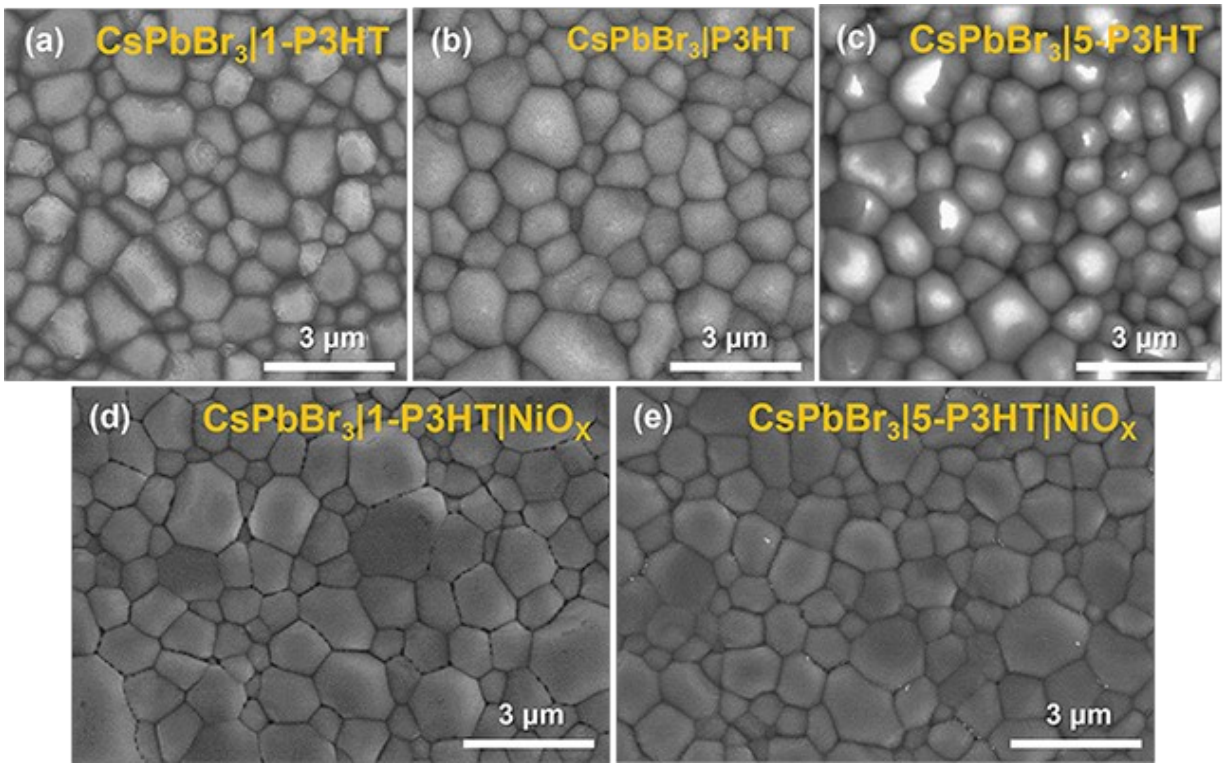

Figure S8. Top-view SEM images of (a) FTO|SnO_2|$CsPbBr_3$|1 mg mL^{-1} P3HT, (b) FTO|SnO_2|$CsPbBr_3$|2 mg mL^{-1} P3HT, (c) FTO|SnO_2|$CsPbBr_3$|5 mg mL^{-1} P3HT, (d) FTO|SnO_2|$CsPbBr_3$|1 mg mL^{-1} P3HT|NiO_X, (e) FTO|SnO_2|$CsPbBr_3$|5 mg mL^{-1} P3HT|NiO_X films.

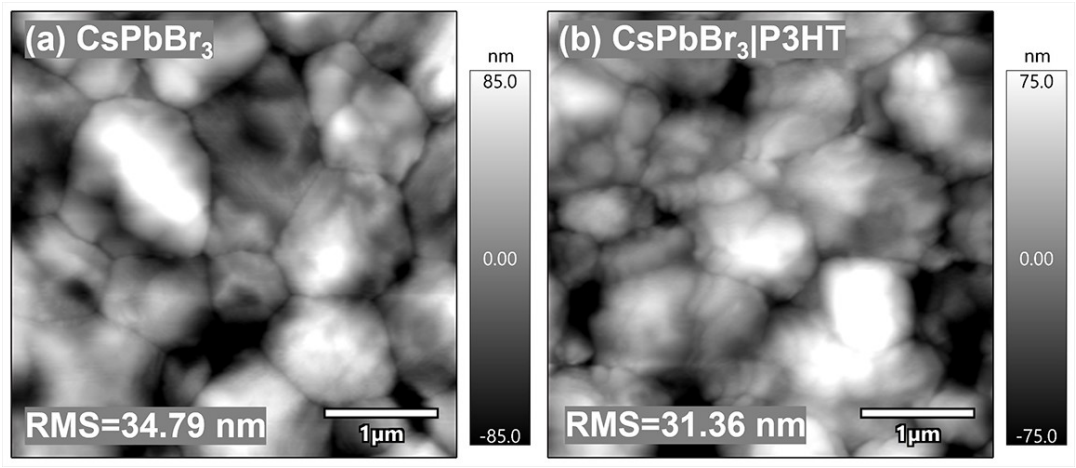

Figure S9. AFM images of (a) FTO|SnO_2|$CsPbBr_3$, (b) FTO|SnO_2|$CsPbBr_3$|2 mg mL^{-1} P3HT films.

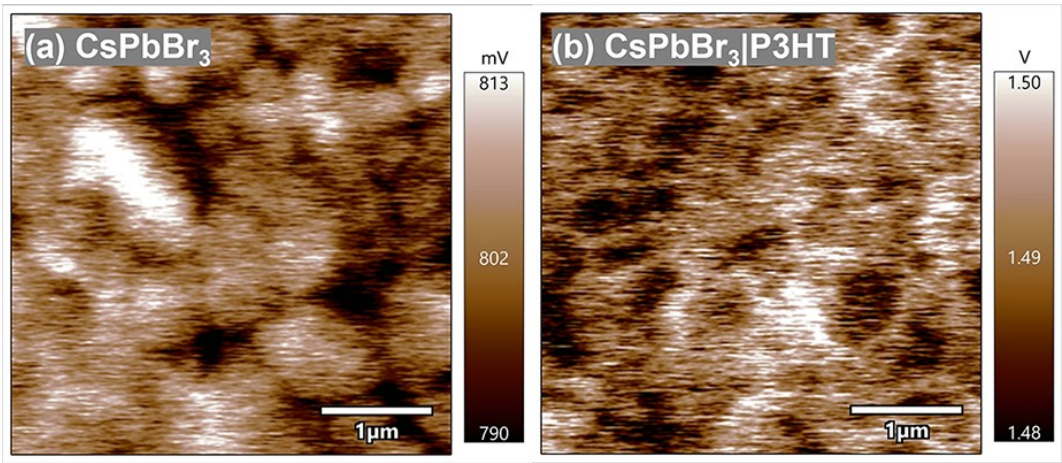

Figure S10. KPFM images of (a) FTO|SnO_2|$CsPbBr_3$, (b) FTO|SnO_2|$CsPbBr_3$|2 mg mL^{-1} P3HT films.

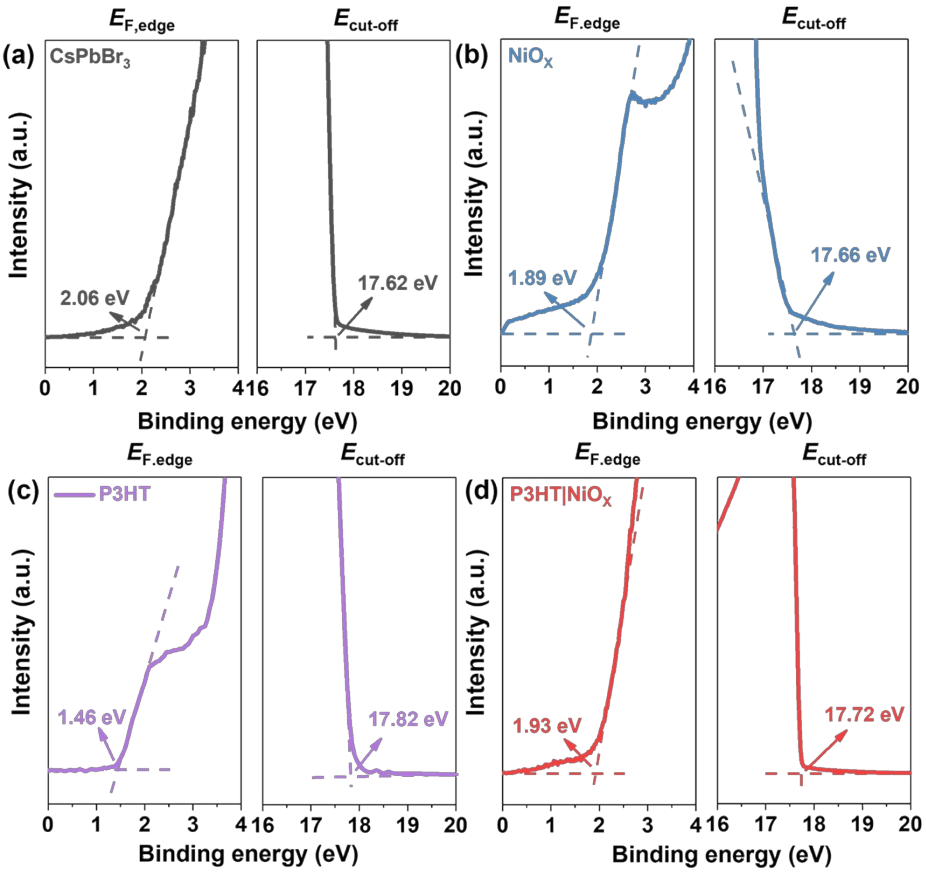

Figure S11. UPS spectra of (a) $CsPbBr_3$, (b) NiO_X, (c) P3HT, and (d) P3HT|NiO_X films, showing the Fermi edge ($E_{F,\,edge}$), and cut-off energy ($E_{cut\text{-}off}$).

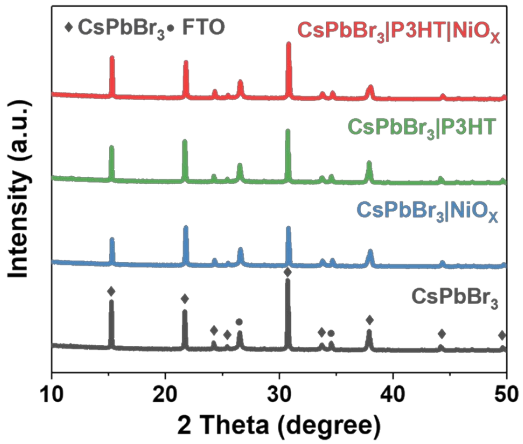

Figure S12. XRD patterns of FTO|SnO_2|$CsPbBr_3$, FTO|SnO_2|$CsPbBr_3$|NiO_X, FTO|SnO_2|$CsPbBr_3$|P3HT, and FTO|SnO_2|$CsPbBr_3$|P3HT|NiO_X films.

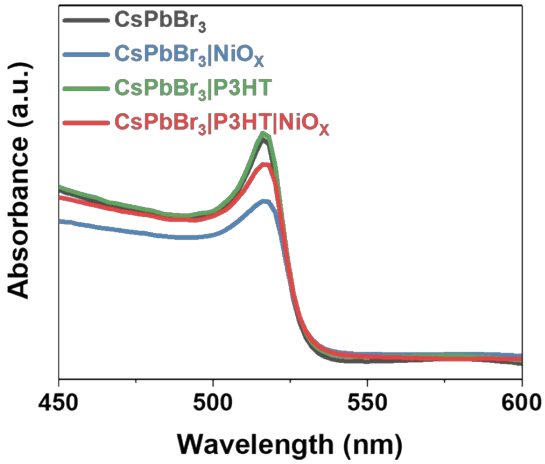

Figure S13. Absorption spectra of FTO|SnO_2|$CsPbBr_3$, FTO|SnO_2|$CsPbBr_3$|NiO_X, FTO|SnO_2|$CsPbBr_3$|P3HT, and FTO|SnO_2|$CsPbBr_3$|P3HT|NiO_X films.

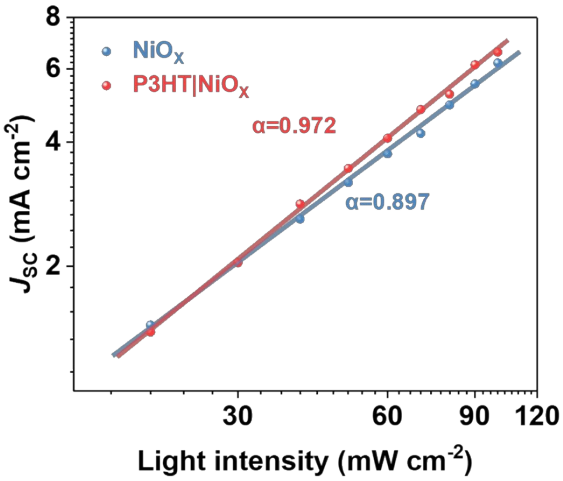

Figure S14. The J_{SC} versus light intensity plots of ST-PSCs with NiO_X or P3HT|NiO_X film.

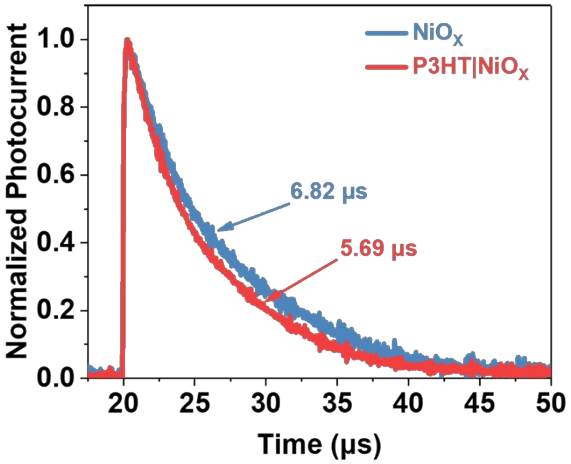

Figure S15. Transient photocurrent (TPC) decay curves of ST-PSCs with NiO_X or P3HT|NiO_X film.

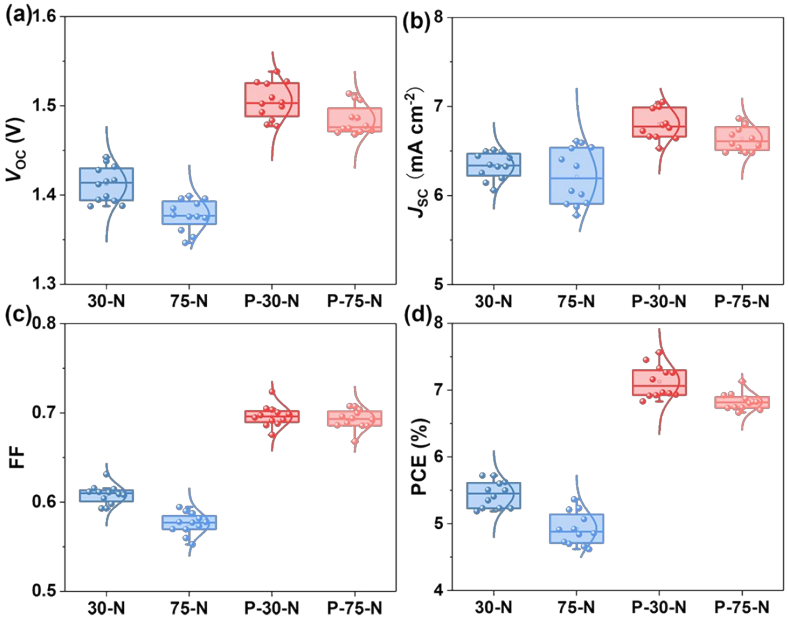

Figure S16. Statistics (a) V_{OC}, (b) J_{SC}, (c) FF, and (d) PCE distributions of 12 independent cells of ST-PSCs with NiO_X or P3HT|NiO_X film prepared by different sputtering powers. These films are fabricated based on 30 W NiO_X (30-N), 75 W NiO_X (75-N), P3HT|30 W NiO_X (P-30-N), and P3HT|75 W NiO_X (P-75-N). All devices were measured under AM 1.5G 1-sun irradiation with a metal mask of 0.16 cm^2.

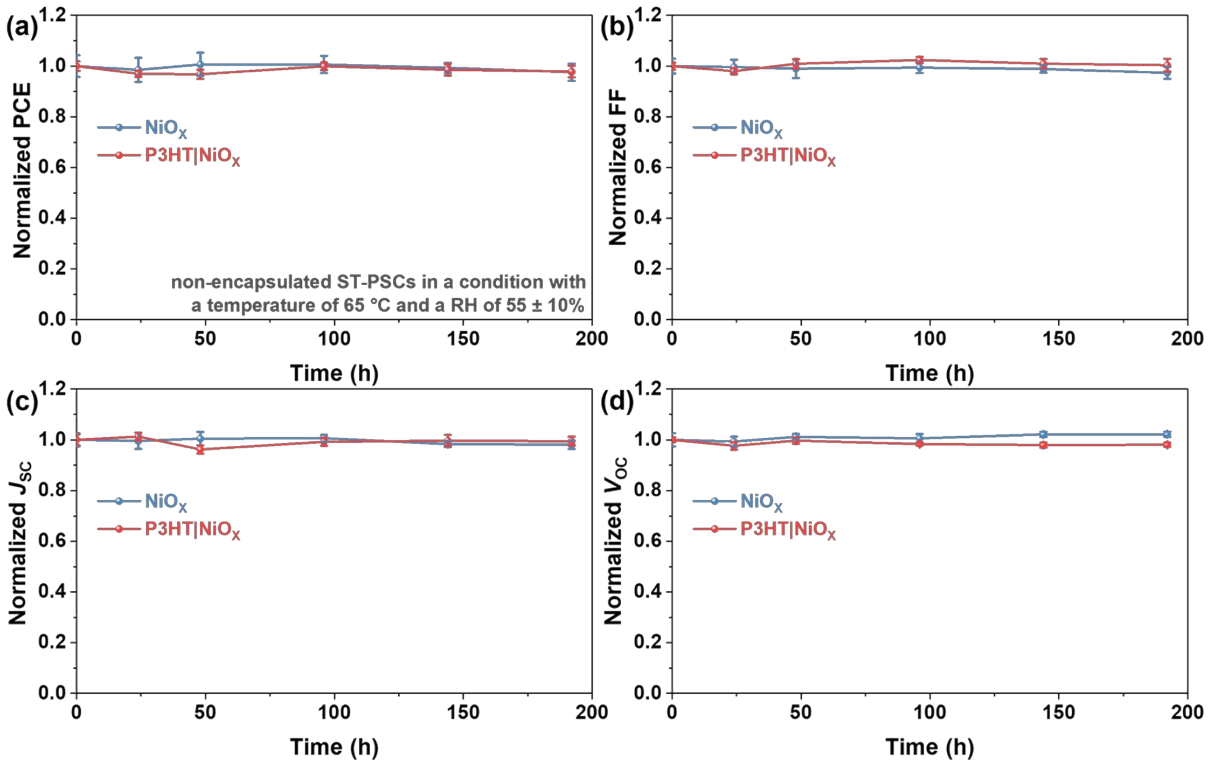

Figure S17. Evolution of (a) PCE, (b) FF, (c) J_{SC}, and (d) V_{OC} originating from non-encapsulated devices with NiO_X or P3HT|NiO_X film aging at a condition with a temperature of 65 °C and a RH of 55 ± 10% in the dark. All devices were measured under AM 1.5G 1-sun irradiation with a metal mask of 0.16 cm^2.

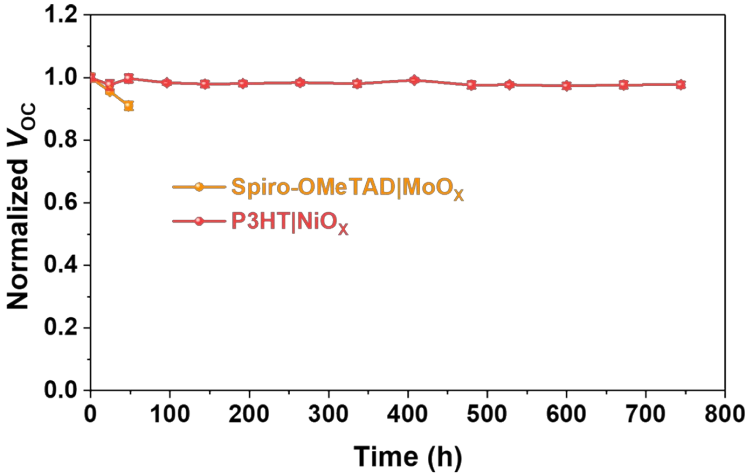

Figure S18. Evolution of V_{OC} originating from non-encapsulated devices with spiro-OMeTAD|MoO_X or P3HT|NiO_X film aging at a condition with a temperature of 65 °C and a RH of 55 ± 10% in the dark. All devices were measured under AM 1.5G 1-sun irradiation with a metal mask of 0.16 cm^2.

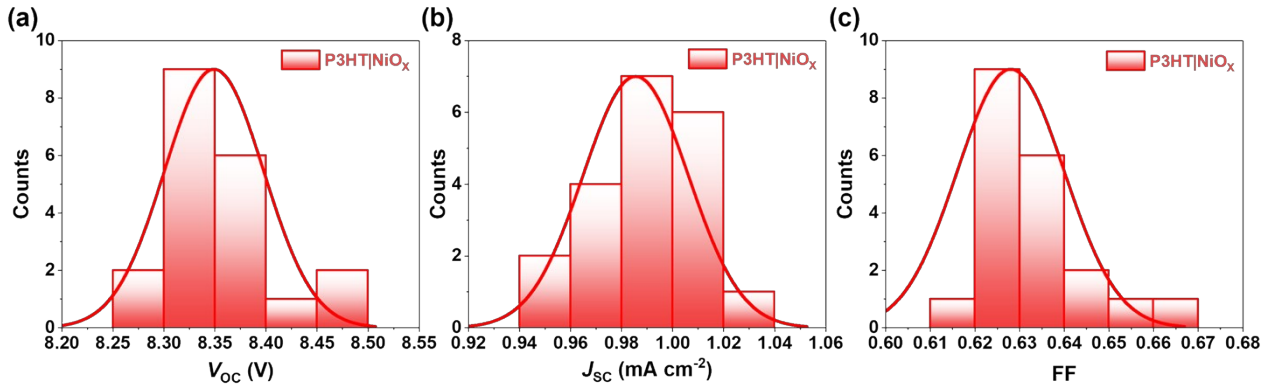

Figure S19. (a) V_{OC}, (b) J_{SC}, and (c) FF distributions of 20 independent modules modification. All modules were measured under AM 1.5G 1-sun irradiation with a metal mask of 10.0 cm^2;

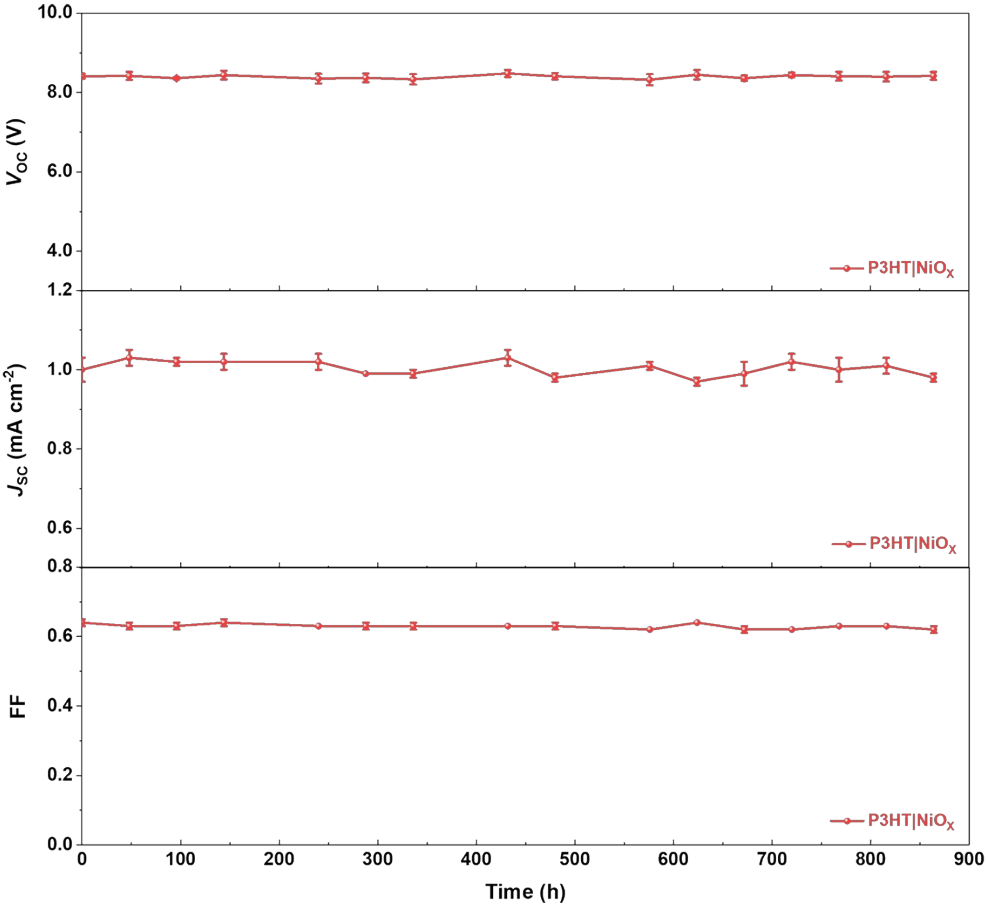

Figure S20. Evolution of V_{OC}, J_{SC}, and FF originating from non-encapsulated modules aging at a condition with a temperature of 25 ± 5 °C and a RH of 35 ± 5% in the dark. All devices were measured under AM 1.5G 1-sun irradiation with a metal mask of 10 cm^2.

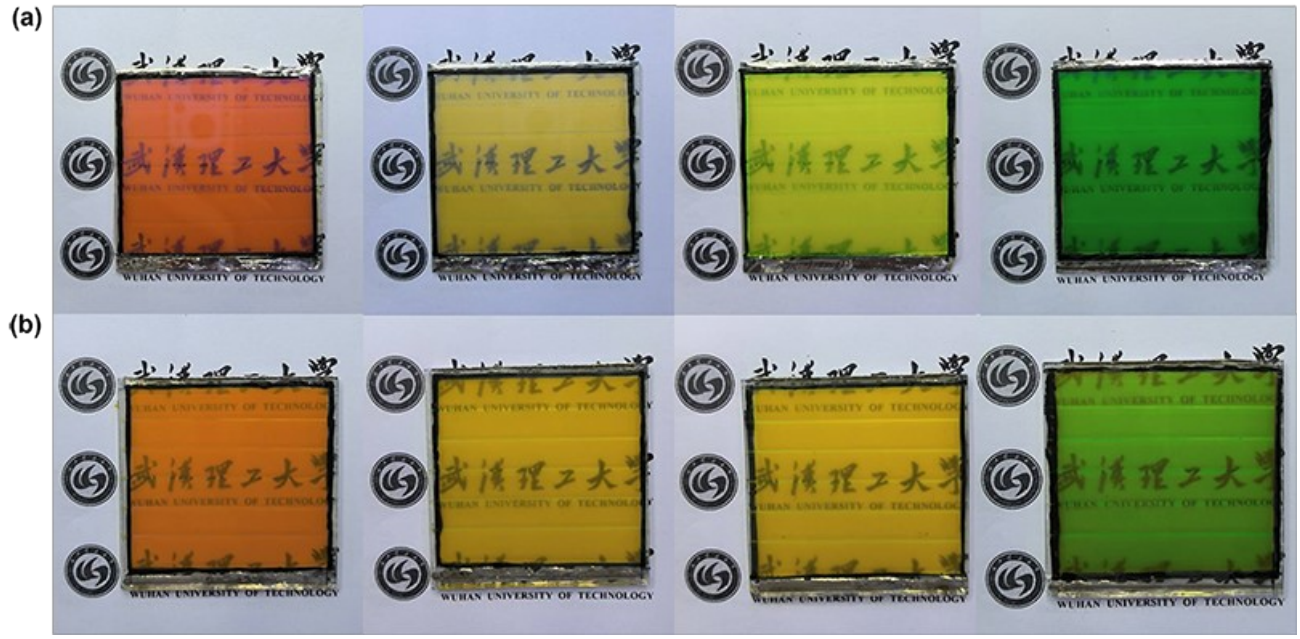

Figure S21. Prototype photos of (a) ordinary glass side and (b) photovoltaic glass side for colorful heat-insulating photovoltaic glass. The device structure is glass|ST-PSM|filter|glass.

Table S1. The atomic ratio of Ni^{2+}/Ni^{3+}, and the value of x in NiO_X with or without annealing under air condition.

Samples	Atomic ratio of Ni^{2+}/Ni^{3+}	The value of x
w/o annealing	0.55	1.32
w/ annealing	0.50	1.33

Table S2. Photovoltaic performance of ST-PSCs based on NiO_X with different annealing temperature. All devices were measured under AM 1.5G 1-sun irradiation with a metal mask of 0.16 cm^2.

Temperature (°C)		V_{OC} (V)	J_{SC} (mA cm^{-2})	FF	PCE (%)
200	Champion	1.33	5.3	0.50	3.6
	Average	1.33 ± 0.02	5.3 ± 0.1	0.48 ± 0.02	3.4 ± 0.2
250	Champion	1.37	6.1	0.53	4.4
	Average	1.37 ± 0.02	5.7 ± 0.2	0.53 ± 0.01	4.2 ± 0.2
300	Champion	1.40	6.5	0.61	5.5
	Average	1.40 ± 0.01	6.5 ± 0.1	0.58 ± 0.02	5.2 ± 0.2
350	Champion	1.37	5.4	0.51	3.8
	Average	1.37 ± 0.02	5.3 ± 0.1	0.49 ± 0.01	3.5 ± 0.2

Table S3. Photovoltaic performance of ST-PSCs based on NiO_X with different annealing time. All devices were measured under AM 1.5G 1-sun irradiation with a metal mask of 0.16 cm^2.

Time (min)		V_{OC} (V)	J_{SC} (mA cm^{-2})	FF	PCE (%)
30	Champion	1.35	6.3	0.53	4.6
	Average	1.37 ± 0.01	5.8 ± 0.3	0.52 ± 0.02	4.2 ± 0.3
60	Champion	1.43	6.5	0.60	5.6
	Average	1.41 ± 0.01	6.4 ± 0.1	0.58 ± 0.01	5.3 ± 0.2
90	Champion	1.42	6.3	0.55	4.9
	Average	1.39 ± 0.02	6.2 ± 0.2	0.55 ± 0.01	4.7 ± 0.2

Table S4. Photovoltaic performance of ST-PSCs based on NiO_X with different thickness. All devices were measured under AM 1.5G 1-sun irradiation with a metal mask of 0.16 cm^2.

Thickness (nm)		V_{OC} (V)	J_{SC} (mA cm^{-2})	FF	PCE (%)
25	Champion	1.39	6.2	0.53	4.6
	Average	1.37 ± 0.02	6.0 ± 0.2	0.51 ± 0.02	4.2 ± 0.3
35	Champion	1.44	6.6	0.62	5.8
	Average	1.41 ± 0.02	6.4 ± 0.2	0.62 ± 0.01	5.6 ± 0.2
45	Champion	1.42	6.2	0.60	5.3
	Average	1.41 ± 0.02	6.2 ± 0.1	0.59 ± 0.01	5.1 ± 0.1

Table S5. Photovoltaic performance, AVT, and LUE of ST-PSCs with spiro-OMeTAD|MoO_X or NiO_X film. All devices were measured under AM 1.5G 1-sun irradiation with a metal mask of 0.16 cm^2.

Samples		V_{OC} (V)	J_{SC} (mA cm^{-2})	FF	PCE (%)	AVT (%)	LUE (%)
Spiro-OMeTAD|MoO_X	Champion	1.48	8.1	0.70	8.4	42.8	3.6
	Average	1.46 ± 0.04	7.8 ± 0.2	0.68 ± 0.02	7.7 ± 0.3		
NiO_X	Champion	1.44	6.5	0.62	5.8	51.3	3.0
	Average	1.43 ± 0.02	6.3 ± 0.1	0.61 ± 0.01	5.6 ± 0.2		

Table S6. Photovoltaic performance of ST-PSCs with different buffer layers. All devices were measured under AM 1.5G 1-sun irradiation with a metal mask of 0.16 cm^2.

Buffer layers		V_{OC} (V)	J_{SC} (mA cm^{-2})	FF	PCE (%)
Pristine	Champion	1.44	6.5	0.62	5.8
	Average	1.43 ± 0.02	6.3 ± 0.1	0.61 ± 0.01	5.6 ± 0.2
1-P3HT	Champion	1.55	6.6	0.67	6.9
	Average	1.50 ± 0.03	6.5 ± 0.2	0.65 ± 0.02	6.3 ± 0.3
2-P3HT	Champion	1.51	6.8	0.69	7.1
	Average	1.52 ± 0.02	6.7 ± 0.1	0.68 ± 0.01	6.9 ± 0.1
5-P3HT	Champion	1.48	6.9	0.65	6.6
	Average	1.39 ± 0.06	7.0 ± 0.3	0.63 ± 0.01	6.2 ± 0.3
PTAA	Champion	1.44	6.1	0.54	4.8
	Average	1.38 ± 0.04	5.9 ± 0.2	0.54 ± 0.02	4.4 ± 0.2
MoO_X	Champion	1.26	6.9	0.47	4.1
	Average	1.27 ± 0.02	6.3 ± 0.3	0.42 ± 0.03	3.4 ± 0.4

Table S7. Calculated valence band (E_{VB}) from $E_{cut\text{-}off}$, and $E_{F,\ edge}$ for the $CsPbBr_3$, NiO_X, P3HT, and P3HT|NiO_X.

Samples	$E_{cut\text{-}off}$ (eV)	$E_{F,\ edge}$ (eV)	E_{VB} (eV)
$CsPbBr_3$	17.62	2.06	-5.66
NiO_X	17.66	1.89	-5.45
P3HT	17.82	1.46	-4.86
P3HT|NiO_X	17.72	1.93	-5.43

Table S8. Fitted results of the TRPL curves of ST-PSCs with NiO_X or P3HT|NiO_X film at short circuit condition.

Samples	A_1	τ_1 (ns)	A_2	τ_2 (ns)	τ_{avg} (ns)*
NiO_X	0.18	1.0	0.82	3.8	3.7
P3HT|NiO_X	0.15	0.8	0.85	2.9	2.8

* τ_{avg} was fitted by the equation: $\tau_{avg} = (A_i\tau_i^2+A_i\tau_i^2)/(A_i\tau_i+A_i\tau_i)$, i=1, 2.

Table S9. The reported results of inorganic ST-PSCs in recent years. (Reverse scan)

Device structures	Perovskite bandgaps (eV)	V_{OC} (V)	J_{SC} (mA cm^{-2})	FF	PCE (%)	AVT (%)	LUE (%)	Ref
ITO|PTAA|PEA-$CsPbI_3$|$PC_{61}BM$|BCP|AZO|ITO	1.78	1.17	10.7	0.78	9.8	31.9	3.1	2
FTO|TiO_2|$CsPbI_3$ PQDs|Spiro-OMeTAD|MoO_X|Au|MoO_X	1.78	1.19	15.0	0.63	11.3	23.4	2.6	3
ITO|ZnO|$CsPbBr_3$|Spiro-OMeTAD|PH1000	2.30	1.38	6.2	0.71	6.0	<43.6	<2.6	4
ITO|SnO_2|$CsPbBr_3$|P3HT|ITO-NPs|Ag-NWs	2.30	1.32	6.3	0.68	5.6	41.6	2.3	5
ITO|P3CT-N|$CsPbI_2Br$|PCBM|C_{60}|BCP|Ag|MoO_X	1.90	1.11	13.2	0.75	11.0	21.2	2.3	6
FTO|SnO_2|$CsPbIBr_2$|Spiro-OMeTAD|MoO_X|Ag|MoO_X	2.08	1.18	8.7	0.69	7.1	29.3	2.1	7
FTO|NiO_X|$CsPbI_{3-X}Br_X$|ZnO|Al-ZnO|ITO	N/A	1.00	7.9	0.59	4.7	35.4	1.7	8
FTO|ZnO|Ni-ZnO|$CsPbBr_3$|Spiro-OMeTAD|ITO	2.30	0.94	15.0	0.35	4.9	35.5	1.7	9
FTO|TiO_2|$CsPbI_2Br$|Spiro-OMeTAD|Ag nanowires	1.90	0.98	10.7	0.65	6.8	22.4	1.5	10
FTO|SnO_2|$CsPbIBr_2$|NiO_X|ITO	2.08	N/A	N/A	N/A	3.9	33.2	1.3	11
FTO|SnO_2|$CsPbBr_3$|Spiro-OMeTAD|MoO_X|ITO	2.35	1.48	8.1	0.70	8.4	42.8	3.6	This work
FTO|SnO_2|$CsPbBr_3$|P3HT|E-beam NiO_X|ITO	2.35	1.51	6.8	0.69	7.1	49.1	3.5	This work

Table S10. Photovoltaic performance of ST-PSCs with NiO_X or P3HT|NiO_X film prepared by different sputtering powers. All devices were measured under AM 1.5G 1-sun irradiation with a metal mask of 0.16 cm^2.

Samples		V_{OC} (V)	J_{SC} (mA cm^{-2})	FF	PCE (%)
30 W NiO_X	Champion	1.44	6.5	0.61	5.7
	Average	1.41 ± 0.02	6.3 ± 0.1	0.61 ± 0.01	5.4 ± 0.2
75 W NiO_X	Champion	1.40	6.5	0.59	5.4
	Average	1.38 ± 0.02	6.2 ± 0.3	0.58 ± 0.01	4.9 ± 0.2
P3HT| 30 W NiO_X	Champion	1.54	6.8	0.72	7.6
	Average	1.51 ± 0.02	6.8 ± 0.2	0.70 ± 0.01	7.1 ± 0.2
P3HT| 75 W NiO_X	Champion	1.51	6.8	0.69	7.1
	Average	1.48 ± 0.02	6.6 ± 0.1	0.69 ± 0.01	6.8 ± 0.1

Table S11. Photovoltaic performance of ST-PSMs with P3HT|NiO_X film. All devices were measured under AM 1.5G 1-sun irradiation with a metal mask of 10 cm^2.

Samples		V_{OC} (V)	J_{SC} (mA cm^{-2})	FF	PCE (%)
P3HT|NiO_X	Champion	8.42	1.0	0.64	5.5
	Average	8.35 ± 0.05	1.0 ± 0.02	0.63 ± 0.01	5.2 ± 0.15

References

1. H. Yin, P. Lv, B. Gao, Y. Zhang, Y. Zhu, M. Hu, B. Tan, M. Xu, F. Huang, Y.-B. Cheng, A. N. Simonov and J. Lu, *J. Mater. Chem. A*, 2022, **10**, 25652-25660.
2. Z. Zhang, R. Ji, X. Jia, S.-J. Wang, M. Deconinck, E. Siliavka and Y. Vaynzof, *Adv. Funct. Mater.*, 2023, 2307471.
3. J. Kim, D. Kim, W. Kim, S. Woo, S.-W. Baek, M. J. Ko and Y. Kim, *Chem. Eng. J.*, 2023, **469**, 143824.
4. W. Chen, J. Zhang, G. Xu, R. Xue, Y. Li, Y. Zhou, J. Hou and Y. Li, *Advanced Materials*, 2018, **30**, 1800855.
5. B. Parida, S. Yoon and D.-W. Kang, *Nanomaterials*, 2021, **11**, 1489.
6. X. Feng, S. Fu, R. Miao, L. Qian, Y. Kong, H. Ji, L. Ai, J. Fang, W. Wang and W. Song, *Solar Energy Materials and Solar Cells*, 2022, **240**, 111683.
7. Y. Zhao, R. Ge, J. Zheng, L. Chen, X. Wang, Y. Zheng, L. Zhong, Y. Zhu, X. Xu, G. Xu and X. Xiao, *Energy Technol.*, 2023, **11**, 2300611.
8. J. Lin, M. Lai, L. Dou, C. S. Kley, H. Chen, F. Peng, J. Sun, D. Lu, S. A. Hawks, C. Xie, F. Cui, A. P. Alivisatos, D. T. Limmer and P. Yang, *Nat. Mater.*, 2018, **17**, 261-267.
9. T. Das, R. Nag, N. K. Rana, M. Nayak, R. Paramanik, A. Bera, S. K. Saha and A. Guchhait, *Energy Fuels*, 2023, **37**, 10642-10651.
10. X. Yang, J. Han, W. Ruan, Y. Hu, Z. He, X. Jia, S. Zhang and D. Wang, *Chin. Chem. Lett.*, 2022, **33**, 1425-1429.
11. R. Ge, Y. Zhao, C. Jiang, J. Zheng, L. Chen, Y. Zheng, G. Xu and X. Xiao, *Sci. China Mater.*, 2023, **66**, 3261-3270.